

RSC Advances



This is an *Accepted Manuscript*, which has been through the Royal Society of Chemistry peer review process and has been accepted for publication.

Accepted Manuscripts are published online shortly after acceptance, before technical editing, formatting and proof reading. Using this free service, authors can make their results available to the community, in citable form, before we publish the edited article. This *Accepted Manuscript* will be replaced by the edited, formatted and paginated article as soon as this is available.

You can find more information about *Accepted Manuscripts* in the [Information for Authors](#).

Please note that technical editing may introduce minor changes to the text and/or graphics, which may alter content. The journal's standard [Terms & Conditions](#) and the [Ethical guidelines](#) still apply. In no event shall the Royal Society of Chemistry be held responsible for any errors or omissions in this *Accepted Manuscript* or any consequences arising from the use of any information it contains.



Journal Name

ARTICLE

Direct Cu²⁺ ion-exchanged into as-synthesized SAPO-34 and its catalytic application in the selective catalytic reduction of NO with NH₃

Received 00th January 20xx,
Accepted 00th January 20xx

DOI: 10.1039/x0xx00000x

www.rsc.org/

Xiao Xiang,^{ab} Miao Yang,^a Beibei Gao,^{ab} Yuyan Qiao,^{ab} Peng Tian,^{a*} Shutao Xu,^a Zhongmin Liu^{a*}

Abstract: A facile and direct ion-exchange (DIE) method has been developed to prepare Cu-exchanged SAPO-34s, in which as-synthesized SAPO-34 is used as a precursor. This approach is simple and economical as compared with the conventional multistep ion exchange procedure. The ion exchange behavior of the as-synthesized SAPO-34s is found to be template-dependent. For SAPO-34s templated by smaller amines, they show a better Cu exchange ability than the corresponding NH₄⁺-SAPO-34 and the Cu loadings rise with the increasing template sizes. Coordination between amine and Cu²⁺ in the as-prepared DIE sample is clearly evidenced. However, oversized amine in the CHA cage may cause a failure of the DIE process due to the steric effect. An obvious surface Cu enrichment is observed for the as-prepared DIE sample, which migrates to the interior of the crystals upon calcination. The Cu-SAPO-34 catalyst prepared by DIE method displays excellent performance in the selective catalytic reduction of NO with NH₃ (NH₃-SCR). Its better low-temperature activity as compared with that of the conventional one is likely due to the higher isolated Cu²⁺ amount and surface Cu content. This promising strategy is expected to facilitate the large-scale industrial preparation of NH₃-SCR catalyst.

1. INTRODUCTION

NO_x compounds are harmful emissions from internal combustion diesel engines working at the lean-burn conditions, which could cause serious environmental problems such as acid rain and photochemical smog¹. As the growing environmental concerns and strict regulations on the emissions of diesel-powered vehicles, effective treatment technologies are highly desired to eliminate these harmful exhausts. Currently, selective catalytic reduction of NO_x with ammonia (NH₃-SCR) has become the most promising technique², which is generally integrated with diesel particulate filter (DPF) to constitute a diesel emission control system due to the space limitations. This thus requires a good hydrothermal stability of the NH₃-SCR catalyst in order to tolerate the periodical regeneration of the DPF to burn off the trapped particulate matter (> 650 °C). In recent years, metal-exchanged small-pore molecular sieves³ such as Cu/SAPO-34⁴ and Cu/SSZ-13⁵ have attracted great attention due to their excellent long-term durability under hydrothermal conditions and high NO_x conversions to N₂ over a relatively wide temperature range as compared with oxide catalysts and other zeolite-based catalysts (Cu/Beta⁶, Fe/Beta⁷, etc.).

Both SAPO-34 and SSZ-13 have the same CHA topology, comprised of cylinder-like cages (0.67×0.67×1.0nm) with 8-membered ring openings (0.38×0.38nm). Aluminosilicate H-SSZ-13 generally has limited high-temperature hydrothermal stability, often accompanying with a dealumination phenomenon. The introduction of Cu²⁺ into the ionic site could stabilize the Si-O-Al bond, enhance the hydrothermal stability, and bring good NH₃-SCR activity⁸. For silicoaluminophosphate molecular sieve SAPO-34, it has excellent high-temperature hydrothermal stability, but its drawback is also obvious. H-SAPO-34 is sensitive to H₂O below 100 °C⁹. Exposure to humid air at room temperature may cause irreversible structure damage arising from the hydrolysis of acidic Si-O-Al bond (the concrete hydrolysis degree depends on the Brønsted acid concentration and the crystal size of H-SAPO-34)¹⁰. Introducing ions such as NH₄⁺ and Cu²⁺ in H-SAPO-34 could evidently improve its tolerance to H₂O at low temperature due to the effective protection of negative framework by those cations.^{11,9b}

Up to date, the most conventional method to prepare Cu-exchanged molecular sieve catalysts is aqueous solution ion exchange. That is, the as-synthesized material is first calcined to remove the organic template, then converted to its NH₄⁺ form, and exchanged with Cu²⁺ ion solution which is followed by a drying and calcination process^{4a}. However, for SAPO molecular sieves, the wet ion exchange would have a risk of structural deterioration because of the high sensitivity of the SAPO frameworks to H₂O at low temperatures. Special attentions should be paid to the ammonium ion exchange process of H-SAPO molecular sieves, though high-quality Cu-

^a National Engineering Laboratory for Methanol to Olefins, Dalian National Laboratory for Clean Energy, Dalian Institute of Chemical Physics, Chinese Academy of Sciences, Dalian 116023, P. R. China;

^b University of Chinese Academy of Sciences, Beijing 100049, P. R. China. etc.

* E-mail: tianpeng@dicp.ac.cn; liuzm@dicp.ac.cn

DOI: 10.1039/x0xx00000x

SAPO-34 catalysts have been reported¹². Gao and Peden once investigated the aqueous ion exchange of H-SAPO-34 and found that H-SAPO-34 synthesized with different templates underwent different extent of structural damage via irreversible hydrolysis^{4a}. High Si content (Si-O-Al bond density) within the samples and framework stress may cause more irreversible hydrolysis. Given that H-SAPO-34 with higher acid densities has higher NO conversion at low temperature and can inhibit NH₃ oxidation reaction in the high temperature range¹², it is desirable to find a simplified and effective way to prepare Cu-exchanged high-Si SAPO-34 while keeping their structure well. In addition, chemical vapor deposition^{4c} and solid-state ion exchange¹³ have also been explored to prepare Cu-exchanged molecular sieves. But pitifully, the obtained catalysts generally contain less isolated Cu²⁺ and show inferior NH₃-SCR activity. Recently, a one-pot method has been reported to synthesize Cu-SSZ-13 by using cheap copper complex as the structure-directing agent¹⁴. The highest Si/Al ratio of one-pot Cu-SSZ-13 is 7.5 and the Cu content is generally higher than 8 wt%. Cu-SAPO-34 and Cu-SAPO-18 have also been synthesized by one-pot method¹⁵. The synthetic conditions should be carefully controlled to obtain products with good purity and lower Cu content in order to achieve good NH₃-SCR activity.

In the present work, a facile and direct method to prepare Cu-exchanged SAPO molecular sieves without the risk of structural damage has been developed by simply contacting the as-synthesized SAPO molecular sieves with Cu²⁺ aqueous solution, which is herein designated as direct ion exchange (DIE) in order to distinguish with the conventional ion exchange (CIE). It is well acknowledged that the as-synthesized molecular sieves, in which the pores and cages are occupied/blocked by organic amines (the negative Si-O-Al bonds are balanced by protonated amines), are more resistant to the acidic/basic post-treatment as compared with its calcined form. However, the direct use of as-synthesized SAPO molecular sieves for ion exchange remains unexplored up to now. This is possibly due to the consideration that the channels are small and blocked by the amines which may restrict the diffusion of metal ions into the crystals.

We choose two high-silica SAPO-34 samples templated by diethylamine (DEA) and triethylamine (TEA) respectively, to demonstrate the feasibility of the present method. Detailed characterizations are performed in order to reveal the inner rules and limitations associated with the DIE method. Finally, we will show that this approach is not restricted to SAPO-34 and Cu²⁺ ion. Other SAPO molecular sieves and metal ions may also have the possibility to employ DIE method for the preparation of metal-exchanged SAPO catalysts.

2. EXPERIMENT

2.1 Zeolite synthesis

SAPO-34 templated by diethylamine (DEA) was synthesized with a starting gel composition of 2.0DEA / 1.0Al₂O₃ / 1.0P₂O₅ / 0.8SiO₂ / 50H₂O. The detailed procedure was as follows: 7.57g

pseudo-boehmite (72.5 wt%) was first mixed with 38.56g water in a beaker. 12.42g phosphoric acid (85 wt%), 8.60g silica sol (30.1 wt%) and 7.88g DEA were added in sequence into the beaker under stirring. The mixture was stirred at room temperature for about 30 min and then transformed into a stainless steel autoclave, which was heated to 200 °C within 60 min and kept at this temperature for 24 h under tumbling. After crystallization, the product was filtered, washed and dried in air.

SAPO-34 templated by triethylamine (TEA) was synthesized with a starting gel composition of 3.0TEA / 1.0Al₂O₃ / 1.0P₂O₅ / 0.8SiO₂ / 50H₂O (200 °C, 48h). The procedure was similar as above except ethylsilicate (TEOS) was used as the Si source.

SAPO-34 templated by N,N,N',N'-tetramethylethylenediamine (TMEDA) was synthesized with a starting gel composition of 7.0TMEDA / 1.2Al₂O₃ / 0.9P₂O₅ / 1.0SiO₂ / 14.6H₂O (200 °C, 48h). The synthetic procedure was similar as that of SAPO-34-DEA.

SAPO-35, SAPO-56 and DNL-6 were prepared with gel compositions of 1.2hexamethylenimine (HMI) / 1.0Al₂O₃ / 1.0P₂O₅ / 0.5SiO₂ / 50H₂O (200 °C, 24h), 2.0N,N,N',N'-tetramethyl-1,6-hexanediamine (TMHD) / 1.0Al₂O₃ / 1.0P₂O₅ / 0.8SiO₂ / 50H₂O (200 °C, 24h) and 2.0DEA / 1.0Al₂O₃ / 1.0P₂O₅ / 0.4SiO₂ / 0.1CTAB / 100H₂O (200 °C, 24h), respectively. The detailed synthetic procedure was similar as above except TEOS and aluminium isopropoxide were used as the Si and Al sources for the synthesis of DNL-6.

SSZ-13 was synthesized according to the literature reported¹⁶. The gel composition was N,N,N-trimethyl-1-adamantammonium (TMAOH) / TEOS / Al(OH)₃ / H₂O = 60 / 100 / 6 / 3100. In details, 17.36g TEOS was first mixed with 0.39g Al(OH)₃, and then 42.28g TMAOH (25%) and 14.5g H₂O were added into the mixture under stirring. The resulting gel was aged at room temperature for 24h before transferred into an autoclave. The autoclave was heated at 160 °C for 4 days under tumbling. After crystallization, the solid product was recovered by filtration, washed, and dried in air.

2.2 Catalyst preparation

The Cu-CHA catalysts were prepared by conventional ion exchange and direct ion exchange methods respectively. For the CIE method, the as-synthesized zeolite was first calcined at 600 °C for 2h to remove the template and water molecules occupied the pores and cages. The calcined zeolite was exchanged with NH₄NO₃ solution (3.66 mol/L) at a liquid-to-solid ratio of 10mL/1g under stirring (80 °C, 2h). The slurry was filtered, washed with deionized water for three times and dried overnight at 100 °C. The obtained NH₄⁺ form zeolite was then exchanged with a solution containing target ions at 50 °C for 4h, which was followed by a filtration, washing and drying procedure. To get the final catalyst, the sample was further calcined at 700 °C for 3h.

The DIE method was simple as compared with the CIE method. No previous calcination and NH₄⁺ exchange processes were required. The as-synthesized zeolite was directly put into the solution containing target ions and stirred at 50 °C for 4h.

Afterwards, the solid was separated, washed, dried at 120 °C and calcined at 700 °C to obtain the catalyst.

2.3 Characterization

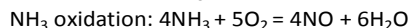
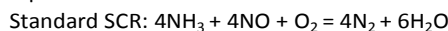
The elemental composition of the samples was determined by XRF (PANalytical Axios advanced). Brunauer–Emmett–Teller (BET) surface areas and pore volumes were measured on Micromeritics ASAP2020, the sample was dehydrated under vacuum at 350 °C for 4h, prior to analysis. All the solid-state NMR experiments were performed on a Bruker Avance III 600 spectrometer equipped with a 14.1 T wide-bore magnet using a 4 mm probe. The resonance frequencies was 600.13 MHz for ¹H. Before ¹H MAS NMR experiment, the samples were dehydrated typically at 420 °C and a pressure below 10⁻³ Pa for 20 h. ¹H MAS NMR spectra were recorded using a single pulse sequence with a $\pi/4$ pulse of 2 μ s and a 10 s recycle delay, with adamantane (1.74 ppm) as the chemical shift reference. For Brønsted acid density quantification, all samples were weighed and their ¹H MAS NMR spectra were resolved by Dmfit software with Gaussian-Lorentz line shapes, using adamantane as the quantitative external standard, measured under the same NMR acquisition condition.

H₂-TPR was performed on Micromeritics Auto Chem II. About 0.15 g sample was pretreated at 550 °C for 1h in argon and then cooled to 100 °C. The TPR procedure was conducted from 100 to 700 °C at a rate of 10 °C /min under 10% H₂/Ar (30 mL/min). The consumption of H₂ was detected by a TCD detector. TG was measured on a TA thermal analyzer SDT Q 600. The sample was heated from room temperature to 1000 °C at a rate of 10 °C/min under flowing air (100 mL/min). To precisely determine and compare the template content of SAPO-34 and Cu-SAPO-34, SAPO-34 was also pretreated in water at the same temperature and solid/liquid ratio as the Cu²⁺ ion exchange before thermal analysis. EDX was conducted on a Hitachi SU8020 equipped with a Horiba X-max silicon drift X-ray detector. XPS was measured on a Thermo ESCALAB 250Xi using a Al K α X-ray source operated at 200 W. The binding energies were corrected referencing to Si 2p (103.4eV). EPR was performed on Bruker A 200. The sample was degased at 100 °C under pressure of 10 um Hg for 7 h before test, and then sealed into a quartz tube for characterization. During spectral collection, microwave power was 10 mW, and frequency was 9.31 GHz. The sweep width was 2000G and sweep time was 84 s, modulated at 100kHz with a 3G amplitude. A time constant of 40ms was used. The spectrum was collected at room temperature. Quantification of isolated Cu²⁺ was conducted by using copper sulfate solution as standard (at -196 °C). Diffuse reflectance UV-Vis spectra were recorded in the range of 200-800 nm against a BaSO₄

reference standard on a VARIAN Cary-5000 UV-Vis-NIR spectrophotometer equipped with an integration sphere.

2.4 Catalytic activity testing

Standard SCR and NH₃ oxidation reaction were performed to evaluate the catalytic behavior of catalysts. The stoichiometric equation of each reaction was:



The standard SCR reaction was conducted at atmospheric pressure in a quartz fixed-bed reactor with an internal diameter of 12 mm. 0.1 g calcined catalyst in 60-80 mesh was diluted with 0.4 g quartz (60-80 mesh). The mixture was fixed in the quartz tube with quartz wool. The catalyst was pretreated with N₂ at 600 °C for 40 min and then cooled to the reaction temperature. The feed gas containing 500 ppm NH₃, 500 ppm NO, 5% O₂, 5% H₂O and balance N₂ was then introduced in the reaction system (water vapor was provided by a saturated tube with a liquid-circulating thermostat water bath). The total flow gas for the reaction was 300 mL/min which corresponded to a GHSV of 180,000 h⁻¹. FTIR spectrometer (BRUKER TENSOR 27) equipped with a gas cell was used to measure the concentrations of NO, NO₂, N₂O and NH₃. At each reaction temperature, at least 30 minutes was kept to ensure the achievement of a steady state.

NH₃ oxidation was performed at the same conditions as standard SCR reaction except the absence of NO in the feed gas.

3. RESULTS AND DISCUSSION

Table 1 gives the physicochemical information of the CHA-type precursors used in the present work. XRD patterns of the precursors and the corresponding Cu ion-exchanged samples are displayed in Fig. S1. The concrete ion exchange conditions, copper contents and template contents in the exchanged products are summarized in Table 2.

Both as-synthesized SAPO-34-DEA and SAPO-34-TEA show the ability to extract Cu ions into their crystals, demonstrating the feasibility of the present DIE method. The Cu loadings in the products are tunable by changing the liquid/solid ratios and exchange number, similar to those observed with the conventional CIE method. It is interesting to note that the DIE samples possess higher Cu content than their corresponding control samples prepared by CIE method (1.3 wt% Cu-DEA-D3 vs. 1.02 wt% Cu-DEA-C1, 1.55 wt% Cu-TEA-D1 vs. 1.02 wt% Cu-TEA-C1), suggesting the better exchange ability of the as-synthesized SAPO-34. Moreover,

Table 1. Physicochemical properties of the precursors used for the ion exchange

Precursor	Product Composition ^a	Acid density (mmol/g) ^b	Template content (wt%) ^c
SAPO-34-DEA	Si _{0.21} Al _{0.46} P _{0.33}	1.48	10.2
SAPO-34-TEA	Si _{0.17} Al _{0.45} P _{0.38}	1.31	12.6
SSZ-13	Si/Al=11.3	-	-

^a Determined by XRF. ^b The Brønsted acid density determined by ¹H MAS NMR. ^c Template content% = $W_{\text{template}} \times 100 / (100 - W_{\text{water}})$, W_{water} and W_{template} are the weight loss in the TG curve in the range of RT – 250 and 250 – 700 °C respectively.

Journal Name

ARTICLE

Table 2. Ion exchange condition, Cu content and template content of Cu-CHA samples

Template	Sample	L/S ^a	Cu content (wt%) ^b	Template content (wt%) ^c	Preparation method
DEA	Cu-DEA-D1	10	0.78	8.9	DIE
	Cu-DEA-D2	15	1.16	8.4	DIE
	Cu-DEA-D3	18	1.3	-	DIE
	Cu-DEA-D4	20	1.41	8.6	DIE
	Cu-DEA-D5	40	2.32	8.3	DIE
	Cu-DEA-C1 ^d	18	1.02	-	CIE
	Cu-DEA-C2 ^d	30	1.38	-	CIE
TEA	Cu-TEA-D1	20	1.55	12.5	DIE
	Cu-TEA-D2	20	2.38	12.5	DIE for two times
	Cu-TEA-C1 ^d	20	1.02	-	CIE
TMAdaOH	Cu-SSZ13-D1	18	0.14	-	DIE
	Cu-SSZ13-C1 ^d	30	1.58	-	CIE

^a The liquid(mL)/solid(g) ratio for Cu ion exchange (0.01 mol/L Cu(OAc)₂ solution, 50 °C, 4h). ^b Determined by XRF. ^c Template content% = $W_{\text{template}} \times 100 / (100 - W_{\text{water}})$, W_{water} and W_{template} are the weight loss in the TG curve in the range of RT – 250 and 250 – 700 °C respectively. ^d The exchange condition for the NH₄⁺-form precursor: 3.66 mol/L NH₄NO₃ solution, 80 °C, 2h.

the as-synthesized SAPO-34 templated by different amines show different ion exchange behavior, when comparing the Cu content in Cu-DEA-D4 (1.41 wt%) and Cu-TEA-D1 (1.55 wt%) prepared by the same exchange protocols. In principle, the ion exchange properties of zeolites are determined by many factors such as crystal sizes and acid density. Herein, considering the same Cu loading for their control samples Cu-DEA-C1 and Cu-TEA-C1 utilizing NH₄⁺-SAPO-34 as the precursor, it is reasonable to claim that the as-synthesized SAPO-34 templated by TEA has a stronger Cu ion exchange ability. Consequently, a sequence about the easiness of amine cations exchanged by Cu ions can be outlined: (C₂H₅)₃NH⁺ > (C₂H₅)₂NH₂⁺ > NH₄⁺. This order is in line with the cationic size. It is supposed that bigger template molecules have weaker electrostatic interaction with the framework due to the steric hindrance effect and thus lead to better ion-exchange behavior. However, this is not always true that the bigger the better. When as-synthesized SSZ-13 (having the same CHA topology as SAPO-34) templated by TMAdaOH was employed as the precursor, only very low Cu loading (0.14 wt% Cu-SSZ13-D1) can be observed, which is obviously lower than that of the CIE sample Cu-SSZ13-C1. In this case, the large TMAda⁺ may occupy most of the CHA cage, block the entrance of Cu ions, and cause the ineffectiveness of the DIE method.

From the above results, it is suggested that the DIE behavior of one molecular sieve is template-dependent, which is determined by the relative sizes of microporosity, template molecules and metal ions. Smaller template molecules

(relative to the cages/channels) are more beneficial for the direct Cu²⁺ exchange, though larger templates having weaker interactions with the framework may lead to a higher metal loading. If oversized template is employed such as TMAda⁺ in SSZ-13, it would cause a failure of the DIE process due to the diffusion limitation of Cu²⁺ into the crystals. Moreover, it is noted that the DIE method should be more applicable to SAPO molecular sieves than to aluminosilicate zeolites for the preparation of deNOx catalyst. The latter generally contains both alkaline ions and organic template. Although the DIE procedure may succeed for zeolites, the calcined DIE sample having both Cu²⁺ and alkaline ions is not suitable for the deNOx reaction due to the occupation of acid sites by alkaline ions.

The thermal analysis results given in Table 1 and Table 2 indicate that the mass percentage of DEA in the as-prepared Cu-SAPO-34-DEA (samples Cu-DEA-D1 ~ Cu-DEA-D5) decreases as compared with that in the precursor, meaning that small amount of DEA escapes from the crystals during the ion exchange. But no linear relationship could be found between the Cu loadings and the weight losses. For the as-prepared Cu-SAPO-34-TEA samples, the organic contents remain almost unchanged before and after the DIE, which implies that larger template can readily stay in the CHA cage during the DIE process.

The textual properties of the selected samples are presented in Table 3. Cu-DEA-D3 exhibits high surface area (501 m²/g) and large micropore volume (0.24 cm³/g), which are just slightly lower than those of the precursor and confirm

the good crystallinity of the Cu-exchanged samples. It is important to note that using higher concentration of NH_4NO_3 solution during the first exchange step of the CIE process is essential to maintain the structural integrity of H-SAPO-34. Otherwise, an obvious drop in the surface area and pore volume (Cu-DEA-C2 vs. NH_4^+ -DEA-T1 and -T2 in Table 3) would

occur due to the partial hydrolysis of the H-SAPO-34 framework^{4a}. Fortunately, there is no such worry about the DIE process. That is, DIE method provides a facile approach to prepare Cu-SAPO-34 catalyst with tunable Cu content and good structural integrity, in which as-synthesized SAPO molecular sieve is directly used as the precursor.

Table 3. Textual properties of the calcined SAPO-34 and Cu-SAPO-34 samples.

Sample	Surface area (m^2/g)		Pore volume (cm^3/g)	
	S_{BET}	S_{micro}	V_{micro}	V_{total}
SAPO-34-DEA	525	515	0.25	0.29
Cu-DEA-D3	501	496	0.24	0.27
Cu-DEA-C2	508	504	0.25	0.28
NH_4^+ -DEA-T1 ^a	191	175	0.09	0.12
NH_4^+ -DEA-T2 ^a	402	391	0.19	0.23

^a NH_4^+ -DEA-T1 and NH_4^+ -DEA-T2 are obtained by exchanging the calcined SAPO-34-DEA with 0.1 and 0.5 mol/L NH_4NO_3 solution at 80 °C for 2 h (liquid/solid ratio = 10 mL / 1 g) respectively.

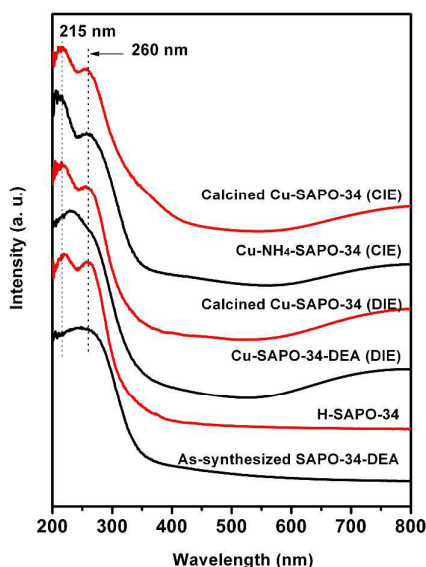


Fig. 1. The UV-Vis spectroscopy results of the samples.

To explore the chemical state and coordination environment of copper species in the samples, UV-Vis spectra are collected and presented in Fig. 1. Both the as-synthesized SAPO-34-DEA and H-SAPO-34 show obvious absorption in the range of 200-300 nm which can be attributed to charge transfer band of the SAPO framework. The existence of splitting peaks observed for H-SAPO-34 should be due to the changes of the SAPO microstructure resulting from high-temperature calcination. After Cu ion exchange, an increase of the signals around 231 and 215 nm can be discerned for the as-prepared DIE and CIE samples respectively. Meanwhile, a new broad band appears in the range of 600-800 nm. According to the literatures, the signal at lower wavelength is attributable to ligand-to-metal charge transfer (LMCT) from the oxygen to isolated $\text{Cu}^{2+}/\text{Cu}^{+17}$ and the absorption at higher wavelength should arise from d-d transitions of Cu^{2+17a} . The difference in the LMCT band position

of the as-prepared DIE and CIE samples suggests that the chemical environments of Cu ions in the two samples are different and the organic amine in the confined CHA cage of the DIE sample may generate coordination with Cu ions. In principle, the nitrogen has higher electron donating ability than the oxygen. However, the steric hindrance with the DEA molecules may increase the distance of the N and Cu^{2+} and thus lead to red shift of the signal from 215 to 231 nm. Indeed, pure Cu-amine complex in SAPO molecular sieves shows an absorption at higher wavelength of $\sim 280 \text{ nm}^{15, 18}$, consistent with our speculation on the partial coordination of Cu ions with DEA. After further calcination, less change occurs for the CIE sample. The spectrum of the DIE sample turns to resemble that of the CIE sample, which indicates the similar Cu^{2+} chemical environments in the two calcined samples.

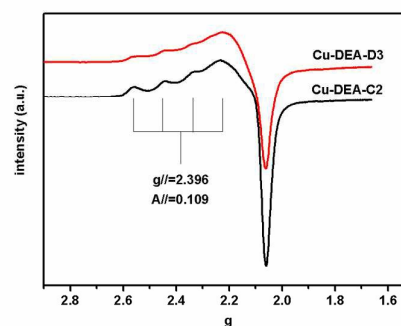
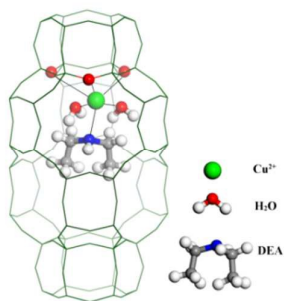


Fig. 2. The EPR spectra of the as-prepared Cu-DEA-D3 and Cu-DEA-C2.

EPR spectra of the as-prepared samples are shown in Fig. 2. Clearly, Cu-DEA-D3 and Cu-DEA-C2 give similar EPR profiles, in which only one type of Cu species with signals of $g// = 2.396$ and $A// = 0.109$ can be determined. It implies that the isolated Cu^{2+} ions in both samples are in similar chemical environments, which dominantly locates in site (I) of the CHA cage¹⁹. Basically, the Cu^{2+} ions in site (I) for hydrated samples have an axial symmetry and octahedrally coordinate to three framework oxygen atoms and three water molecules^{19a}. Here, for the DIE sample, one water molecule around the coordination sphere

of the Cu^{2+} ion is supposed to be substituted by template molecule according to the above UV-Vis results. A proposed representation on the location and coordination environment of the isolated Cu^{2+} in the as-prepared Cu-SAPO-34-DEA is given in **Scheme 1**. The quantified results for the samples from EPR are summarized in Table 4. The as-prepared CIE sample possesses more isolated Cu^{2+} than the DIE one. However, upon calcination, the Cu^{2+} amount of DIE sample shows an interesting increase, whereas the CIE sample does not change too much. It implies that calcination process is important for the DIE sample to generate more isolated Cu^{2+} ions. The higher Cu^{2+} content on calcined DIE sample is expected to be beneficial to its catalytic performance in the NH_3 -SCR reaction.



Scheme 1. Schematic representation of the possible location and coordination environment of Cu^{2+} in the as-prepared Cu-SAPO-34-DEA. The Cu ion locates in site (I) and coordinates with three framework oxygen atoms, two water molecules and one DEA molecule.

Table 4. Quantified results of Cu^{2+} for the DIE and CIE samples from EPR

	Calcination	Cu loading from XRF (wt%)	Isolated Cu^{2+} from EPR (wt%)	Isolated Cu^{2+} / Cu loading
Cu-DEA-D3	Before	1.30%	0.53%	40.8%
	After	1.30%	1.12%	86.1%
Cu-DEA-C2	Before	1.38%	0.86%	62.3%
	After	1.38%	0.90%	65.2%

XPS can give information about chemical valence and concentration of atoms in the external layer of the materials. Fig. 3 displays the Cu 2p XPS spectra of Cu-DEA-D3 and Cu-DEA-C2. The as-prepared Cu-DEA-D3 and Cu-DEA-C2 show similar spectra with two signals located at 933.18 and 952.98 eV, which are attributable to $\text{Cu } 2p_{3/2}$ and $\text{Cu } 2p_{1/2}$ respectively. It indicates that the copper species on the surface of samples prepared by DIE and CIE methods have similar chemical states. Upon calcination at 700 °C, a sharp decrease of the signals is observed, suggesting the reduced Cu amount on the external surface. This is likely due to the migration of Cu species to the interior of SAPO-34 crystals²⁰. The Cu/Al ratio of each sample is calculated and listed in Table 5. Clearly, the surface Cu/Al ratios for the as-prepared DIE and CIE samples are obviously higher than the bulk determined by XRF, showing that Cu is mainly concentrated in the outer subsurface of the as-prepared Cu-SAPO-34 crystals. After calcination, the Cu

content on the external surface drops sharply and the Cu/Al ratio becomes even lower than that of the bulk, which confirms the inward migration and redistribution of Cu species during the high-temperature calcination and agrees with the literatures²⁰⁻²¹. In addition, it is found that the surface copper concentration on Cu-DEA-D3 is a little higher than on the control sample Cu-DEA-C2, whatever in the as-prepared and calcined forms, meaning that more copper species located at the surface layer of the DIE sample. This phenomenon is possibly related to the slightly steric effect of the templates in the CHA cages.

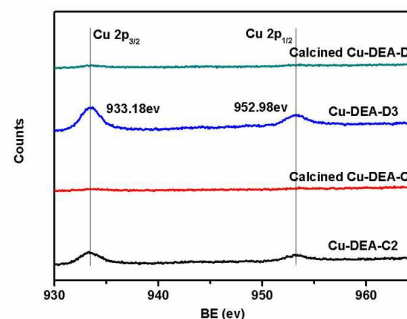


Fig. 3. The Cu 2p XPS spectra of the as-prepared and calcined samples.

Table 5. The bulk and surface Cu/Al atom ratio of the samples

Sample	XRF	XPS	
		As-prepared	Calcined
Cu-DEA-D3	0.028	0.136	0.013
Cu-DEA-C2	0.029	0.108	0.007

EDX was further performed to visualize the dispersion of copper species in the calcined crystals. From Fig. 4, homogeneous copper distribution can be observed and no obvious difference exists between the DIE and CIE samples.

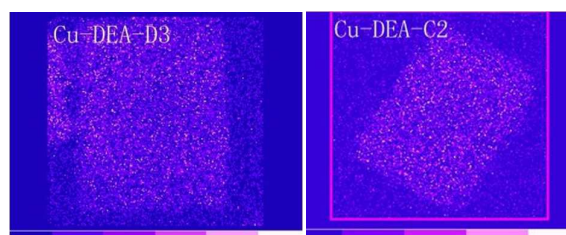


Fig. 4. The EDX images (Cu Ka1) of the calcined samples. The crystal size in the images is about 8 μm .

H_2 -TPR was conducted to distinguish different copper species in the samples (Fig. 5). Comparable profiles with two H_2 consuming peaks around 180-230 and 450-500 °C are perceived for Cu-DEA-D3 and Cu-DEA-C2. The broadness of the peaks together with the weak shoulder at the right side of the high-temperature peaks suggests that multiple Cu species coexist in the samples and their relative concentrations in the two samples is likely similar. According to the literatures, the

formation of CuO_x clusters is inevitable on Cu-SAPO-34 catalyst prepared by CIE method.⁴³ Here we ascribe the low-temperature peak to the reduction of CuO_x particles and the higher one to the reduction of isolated Cu^{2+} ions. The slight downshift of the high-temperature peak observed for the DIE sample is supposed to result from its relatively higher Cu content at the external layer of the crystals as compared with that of the CIE sample.

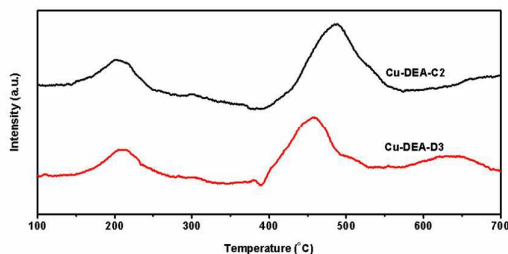


Fig. 5. H_2 -TPR results of Cu-DEA-D3 and Cu-DEA-C2.

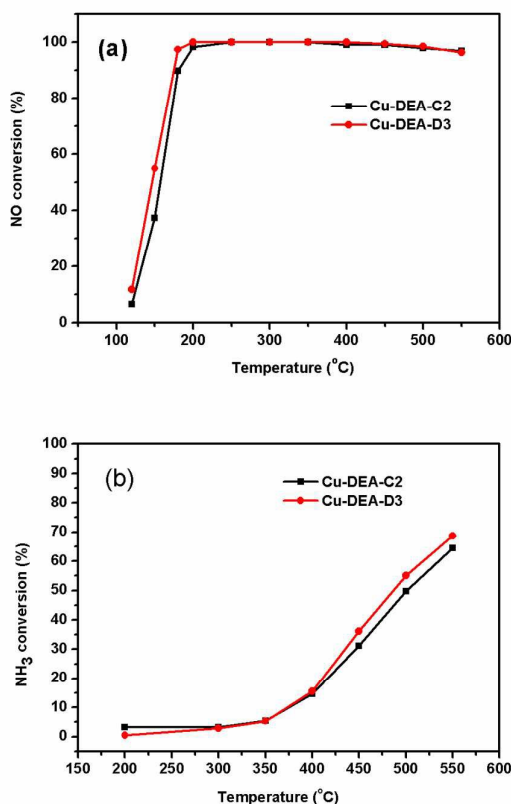


Fig. 6. (a) The standard SCR results with the feed gas of 500 ppm NH_3 , 500 ppm NO , 5% O_2 , and 5% H_2O with N_2 as the balance. (b) The NH_3 oxidation results with the feed gas of 500 ppm NH_3 , 5% O_2 , 5% H_2O with N_2 as the balance. The volume hourly space velocity in all experiments was $180,000 \text{ h}^{-1}$.

One remarkable feature of the present DIE sample is its excellent catalytic performance in the NH_3 -SCR reaction. Fig. 6a displays the NO_x conversion as a function of temperature in

the standard NH_3 -SCR reaction carried out at a GHSV of $180,000 \text{ h}^{-1}$ over Cu-DEA-D3 and Cu-DEA-C2. At lower temperature region ($< 200^\circ\text{C}$), a better activity can be found with the DIE sample (the calculated TOF results of Cu-DEA-D3 shown in Fig. S2 are even higher than that of Cu-DEA-C2). Because intracrystalline diffusion limitations have been discovered to exist in the NH_3 -SCR reaction over Cu-CHA zeolite at low reaction temperatures²², it is supposed that the better low-temperature activity on Cu-DEA-D3 is likely related to its higher surface Cu concentration as revealed by XPS. In addition, the higher isolated Cu^{2+} content in the DIE sample should also make a positive contribution. With the increasing temperature from 200 to 550°C , both the DIE and CIE samples give very similar activity with NO_x conversion of higher than 96%. The slight drop of NO_x conversion observed after 450°C over the catalysts is supposed to result from the nonselective NH_3 oxidation. Fig. 6b gives the NH_3 oxidation results of the catalysts. Both samples display rising activities for NH_3 oxidation with the increasing temperature and just minor difference between the two samples is observed. The higher NH_3 conversion at high temperatures is in consistency with the declining NO_x conversion in standard-SCR reaction at this temperature range.

Besides the success in the preparation of Cu-SAPO-34 catalysts, experiments using other as-synthesized SAPO molecular sieves and metal ions are also explored. As shown in Table 6, it is interesting to find that the DIE method is not limited to SAPO-34 and Cu^{2+} ion. Cu-containing small-pore SAPO-35, SAPO-56 and DNL-6 could be easily prepared by this facile strategy. The Cu loadings on the samples differ from each other, which should result from a combined influence of acid concentration, pore structure and template size. In addition, other metal ions besides Cu^{2+} also show the ability to exchange into the as-synthesized SAPO molecular sieve. Six metal ions including Ni, Ce, Mn, Co, Zn and Ag are investigated here. Under the same exchange conditions, Ce, Zn and Ag ions exhibit better exchanging performance with higher loading amount, whereas Ni and Co ions show inferior behavior. In order to exclude the possibly negative influence of template in the as-synthesized SAPO-34, CIE method using NH_4^+ -SAPO-34 as the precursor is conducted, but even lower Ni and Co loadings are obtained (Table 6). Generally, the metal ions with smaller hydrated diameter are thought to be easier to get through the channel and exchange to the cationic sites. However, this seems not to be the unique factor that governs the exchange behavior, because the hydrated diameters of these ions are close to each other and obviously larger than the pore size of SAPO-34 ($0.38 \times 0.38 \text{ nm}$). It means that the hydrated ions must dissociate part of ligands (H_2O) before it enters into the small pores of SAPO-34. The difference in dissociation energy of various hydrated metal ions may lead to their distinct ion exchange performance. Although the exact reasons need to be further investigated, it is clear that the simple DIE method could be applied to prepare various metal-containing SAPO molecular sieve catalysts.

Table 6. The ion exchange results of different metal ions and SAPO molecular sieves

Matrix	Salt type	L/S ^a	Metal content (wt%)	Ionic diameter ²³ (Å)	Hydrated ionic diameter ²³ (Å)
SAPO-34-DEA	Ce(NO ₃) ₃	30	2.05	2.02	9.04
SAPO-34-DEA	Zn(OAc) ₂	30	1.44	1.48	8.6
SAPO-34-DEA	AgNO ₃	37.5	4.14	2.52	6.82
SAPO-34-DEA	Mn(OAc) ₂	30	0.75	1.6	8.76
SAPO-34-DEA	Ni(NO ₃) ₂	30	0.56	1.4	8.08
SAPO-34-DEA	Co(OAc) ₂	30	0.5	1.44	8.46
SAPO-35-HMI ^b	Cu(OAc) ₂	60	1.0	1.44	8.38
DNL-6-DEA ^b	Cu(OAc) ₂	30	2.35	1.44	8.38
SAPO-56-TMHD ^{b,c}	Cu(OAc) ₂	30	2.23	1.44	8.38
NH ₄ ⁺ -SAPO-34 ^d	Ni(NO ₃) ₂	30	0.1	1.4	8.08
NH ₄ ⁺ -SAPO-34 ^d	Co(OAc) ₂	30	0.31	1.44	8.46

^a The liquid (mL)/solid (g) ratio for ion exchange (0.01 mol/L solution, 50 °C, 4h). ^b The molar compositions of SAPO-35, DNL-6 and SAPO-56 are Si_{0.13}Al_{0.51}P_{0.36}, Si_{0.11}Al_{0.52}P_{0.37} and Si_{0.22}Al_{0.44}P_{0.34} respectively. ^c 0.03 mol/L Cu²⁺ solution is used for the DIE. ^d NH₄⁺-SAPO-34 is prepared using calcined SAPO-34-DEA as the precursor.

Another advantage of the DIE method is that it may be used for selective extraction of metal ion from mixed salt solution as deduced from the above distinct ion-exchange behavior. Herein, as a preliminary trial, a solution containing Cu²⁺, Zn²⁺, Co²⁺, Ni²⁺ ions is employed and the results are displayed in Table 7. Interestingly, the two as-synthesized SAPO-34s show preferential extraction for Cu²⁺. The exchange amounts of Zn²⁺, Co²⁺ and Ni²⁺ are much lower than those of their individual DIE. Particularly for Co²⁺ and Ni²⁺, their loadings are almost negligible. This suggests that the ion exchange behavior of the sample may be modified by the competition caused by the coexistence of multiple cations. The lower loading and higher selectivity to Cu²⁺ observed over high-Si SAPO-34-TMEDA should mainly result from the larger template size in the sample, considering its similar crystal size to that of SAPO-34-DEA²⁴. It is supposed that the ion exchange selectivity of the as-synthesized molecular sieves may be tuned by choosing suitable template and topology type.

Table 7. The ion exchange results of SAPO molecular sieves in mixed salt solution.

Matrix	Metal content in the product (wt%) ^a			
	Cu	Co	Ni	Zn
SAPO-34-DEA	2.13	0.04	0.02	0.41
SAPO-34-TMEDA ^b	0.78	0.01	0.01	0.08

^a The ion exchange solution consists of Cu(NO₃)₂, Co(NO₃)₂, Ni(NO₃)₂ and Zn(NO₃)₂. The concentration of each cation is 0.05mol/L, exchanged at 50 °C for 4h. ^b The molar composition of SAPO-34-TMEDA is Si_{0.18}Al_{0.46}P_{0.36}.

Conclusions

A direct ion-exchange strategy to prepare Cu-SAPO-34 with tunable Cu content and good structural integrity has been developed by simply contacting the as-synthesized SAPO-34 with Cu²⁺ aqueous solution. It is revealed that the ion exchange behavior of the as-synthesized SAPO-34 is template-dependent. SAPO-34s templated by smaller amines display a higher Cu loading than the corresponding NH₄⁺-SAPO-34 and the exchange ability rises with the increasing template size, likely arising from the longer distance and weaker electrostatic interaction of amines with the negative framework. But oversized template in the materials would cause a failure of the DIE process because of the steric hindrance. Coordination between amine and Cu²⁺ in the confined CHA cage is clearly evidenced. XPS results reveal a surface Cu enrichment on the as-prepared DIE sample and high-temperature calcination remarkably prompts the inward migration and redistribution of Cu species. The Cu-SAPO-34 catalyst prepared by DIE method shows excellent catalytic performance in the NH₃-SCR reaction. The better low-temperature activity over DIE catalyst than on CIE catalyst should relate to its higher surface Cu amount and isolated Cu²⁺ content. Interestingly, the DIE method is not limited to SAPO-34 and Cu²⁺ ions, which can be successfully applied to prepare other types of metal-exchanged SAPO molecular sieves and also show potentials for selective extraction of metal ion from mixed salt solution.

Acknowledgements

We are grateful for the financial support from the National Natural Science Foundation of China (NSFC 21476228 and 211011150).

Notes and references

- Roy, S.; Hegde, M. S.; Madras, G. *Applied Energy* 2009, 86 (11), 2283-2297.
- Koebel, M.; Elsener, M.; Kleemann, M. *Catalysis Today* 2000, 59 (3-4), 335-345.
- Fickel, D. W.; D'Addio, E.; Lauterbach, J. A.; Lobo, R. F. *Applied Catalysis B: Environmental* 2011, 102 (3-4), 441-448.
- (a) Gao, F.; Walter, E. D.; Washton, N. M.; Szanyi, J.; Peden, C. H. F. *ACS Catalysis* 2013, 3 (9), 2083-2093; (b) Wang, J.; Yu, T.; Wang, X.; Qi, G.; Xue, J.; Shen, M.; Li, W. *Applied Catalysis B-Environmental* 2012, 127, 137-147; (c) Deka, U.; Lezcano-Gonzalez, I.; Warrender, S. J.; Lorena Picone, A.; Wright, P. A.; Weckhuysen, B. M.; Beale, A. M. *Microporous and Mesoporous Materials* 2013, 166, 144-152.
- Kwak, J. H.; Tran, D.; Szanyi, J.; Peden, C. H. F.; Lee, J. H. *Catalysis Letters* 2012, 142 (3), 295-301.
- Wilken, N.; Nedyalkova, R.; Kamasamudram, K.; Li, J.; Currier, N. W.; Vedaiyan, R.; Yezerets, A.; Olsson, L. *Topics in Catalysis* 2013, 56 (1-8), 317-322.
- Boroń, P.; Chmielarz, L.; Gurgul, J.; Łątka, K.; Gil, B.; Krafft, J.-M.; Dzwigaj, S. *Catalysis Today* 2014, 235, 210-225.
- Gao, F.; Kwak, J. H.; Szanyi, J.; Peden, C. H. F. *Topics in Catalysis* 2013, 56 (15-17), 1441-1459.
- (a) Briend, M.; Vomscheid, R.; Peltre, M. J.; Man, P. P.; Barthomeuf, D. *Journal of Physical Chemistry* 1995, 99 (20), 8270-8276; (b) Mees, F. D. P.; Martens, L. R. M.; Janssen, M. J. G.; Verberckmoes, A. A.; Vansant, E. F. *Chemical Communications* 2003, (1), 44-45.
- Li, Z.; Martinez-Triguero, J.; Concepcion, P.; Yu, J.; Corma, A. *Physical chemistry chemical physics : PCCP* 2013, 15 (35), 14670-80.
- Wang, J.; Fan, D.; Yu, T.; Wang, J.; Hao, T.; Hu, X.; Shen, M.; Li, W. *Journal of Catalysis* 2015, 322, 84-90.
- Yu, T.; Wang, J.; Shen, M.; Li, W. *Catalysis Science & Technology* 2013, 3 (12), 3234.
- Gao, F.; Walter, E. D.; Washton, N. M.; Szanyi, J.; Peden, C. H. F. *Applied Catalysis B: Environmental* 2015, 162, 501-514.
- Ren, L.; Zhu, L.; Yang, C.; Chen, Y.; Sun, Q.; Zhang, H.; Li, C.; Nawaz, F.; Meng, X.; Xiao, F.-S. *Chemical Communications* 2011, 47 (35), 9789-9791.
- (a) Martínez-Franco, R.; Moliner, M.; Corma, A. *Journal of Catalysis* 2014, 319, 36-43; (b) Martínez-Franco, R.; Moliner, M.; Franch, C.; Kustov, A.; Corma, A. *Applied Catalysis B-Environmental* 2012, 127, 273-280.
- Bohström, Z.; Arstad, B.; Lillerud, K. P. *Microporous and Mesoporous Materials* 2014, 195, 294-302.
- (a) Pralialud, H.; Mikhailenko, S.; Chajar, Z.; Primet, M. *Applied Catalysis B-Environmental* 1998, 16 (4), 359-374; (b) Shi, C.; Xu, L.; Zhu, A.; Zhang, Y.; Au, C. T. *Chinese Journal of Catalysis* 2012, 33 (9-10), 1455-1462.
- Martínez-Franco, R.; Moliner, M.; Concepcion, P.; Thogersen, J. R.; Corma, A. *Journal of Catalysis* 2014, 314, 73-82.
- (a) Xue, J.; Wang, X.; Qi, G.; Wang, J.; Shen, M.; Li, W. *Journal of Catalysis* 2013, 297, 56-64; (b) Zamadics, M.; Chen, X. H.; Kevan, L. *Journal of Physical Chemistry* 1992, 96 (6), 2652-2657; (c) Zamadics, M.; Chen, X. H.; Kevan, L. *Journal of Physical Chemistry* 1992, 96 (13), 5488-5491.
- Vennestrøm, P. N. R.; Katerinopoulou, A.; Tiruvalam, R. R.; Kustov, A.; Moses, P. G.; Concepcion, P.; Corma, A. *ACS Catalysis* 2013, 3 (9), 2158-2161.
- (a) Wang, L.; Gaudet, J. R.; Li, W.; Weng, D. *J Catal* 2013, 306, 68-77; (b) Wang, J.; Huang, Y.; Yu, T.; Zhu, S.; Shen, M.; Li, W.; Wang, J. *Catalysis Science & Technology* 2014, 4 (9), 3004-3012.
- Gao, F.; Walter, E. D.; Karp, E. M.; Luo, J.; Tonkyn, R. G.; Kwak, J. H.; Szanyi, J.; Peden, C. H. F. *Journal of Catalysis* 2013, 300, 20-29.
- Nightingale, E. R. *Journal of Physical Chemistry* 1959, 63 (9), 1381-1387.
- Fan, D.; Tian, P.; Su, X.; Yuan, Y.; Wang, D.; Wang, C.; Yang, M.; Wang, L.; Xu, S.; Liu, Z. *Journal of Materials Chemistry A* 2013, 1 (45), 14206.

TOC

